Coastal Engineering 58 (2011) 540–553

Contents lists available at ScienceDirect

Coastal Engineering

journal homepage: www.elsevier.com/locate/coastaleng

Empirical design of scour protections around monopile foundations Part 1: Static approach

Leen De Vos [a,*], Julien De Rouck [a], Peter Troch [a], Peter Frigaard [b]

[a] Ghent University, Dept. of Civil Engineering, Technologiepark 904, 9052 Ghent, Belgium
[b] Aalborg University, Dept. of Civil Engineering, Sohngaardsholmsvej 57, DK-9000 Aalborg, Denmark

ARTICLE INFO

Article history:
Received 7 July 2010
Received in revised form 7 February 2011
Accepted 14 February 2011
Available online 15 March 2011

Keywords:
Monopile
Scour protection
Offshore wind
Design formula
Static stability

ABSTRACT

Together with new opportunities, offshore wind farms raise new engineering challenges. An important aspect relates to the erosion of bottom material around the foundation of the wind turbines, caused by the local increase of the wave and current induced flow velocities by the pile's presence. Typically, the expected scour has a considerable impact on the stability and dynamic behavior of the wind turbine and a scour protection is placed to avoid erosion of the soil close to the foundation. Although much experience exists on the design of scour protections around bridge piers (which are placed in a current alone situation), at present, little design guidelines exist for the specific case of a scour protection around a monopile foundation subjected to a combined wave and current loading.

This paper describes the derivation of a static design formula to calculate the required stone size for a scour protection around a monopile foundation in a combined wave and current climate. Due to the difficult physical processes involved in flow disturbance and displacement of bed protection material at the base of a foundation, the formula is based on the results of an experimental model study which is described in this paper. A linear relationship was found between the critical bed shear-stress τ_{cr} and the bed shear-stress caused by current τ_c and waves τ_w, respectively. When applying the formula for a typical situation in the North Sea, a significant reduction of the required stone size is obtained, compared to existing design criteria. In part 2, following this paper (De Vos et al., in preparation), an optimization of the design procedure is obtained by allowing limited stone motion for top layer stones. This is obtained by adding a damage factor to the design formula, which leads to significantly smaller stone diameters and thus a more economical approach.

1. Introduction

When building offshore wind turbines, the disruption of the flow caused by the presence of the foundation induces local scour at the foundation's base. For a monopile foundation, which is at present the most commonly used foundation type, the scour depth can amount to two times the pile diameter. This seriously affects the stability and dynamical behavior of the foundation (Sumer and Fredsøe, 2002). Virtually in every case of offshore wind farms already built, a scour protection consisting of rip-rap material is chosen for to guarantee the foundation's stability.

As the existing experience has not been reported in literature, little to no formulae are available to calculate the required stone size for a scour protection around a monopole foundation in a combined wave and current climate (Sumer and Fredsøe, 2002). To design and construct the scour protections of existing wind farms, a static approach based on the criteria of the threshold of motion is generally used to calculate the required stone size (e.g. Kirkegaard et al., 1998). A physical scale model study is then used to verify the often conservative design. To the authors' knowledge, very few empirical design methods exist other than the method developed in the OPTI-PILE project from E-Connection et al. (2002–2004).

The static approach design method uses the bed shear-stress, which represents the force per area exerted on the bed by the waves and current and is proportional to the square of the flow velocity. When the bed shear-stress exceeds a threshold value, a grain or rock can be trailed by the current. When the bed shear-stress value decreases, the grain or rock resettles on the bottom. The threshold value is called the critical bed shear-stress and is defined by the stone properties (dimensions and density). The local increase in bed shear-stress caused by the pile's disruption of the flow is quantified by an amplification factor which is applied to the undisturbed bed shear-stress which is present when no pile is installed (Sumer and Fredsøe, 2002). The difficulties in the existing design method lie in the combination of wave and current related bed shear-stresses and in the choice of the amplification factor.

* Corresponding author.
E-mail addresses: Leen.DeVos@mow.vlaanderen.be (L. De Vos), Julien.Derouck@UGent.be (J. De Rouck), Peter.Troch@UGent.be (P. Troch), pf@civil.aau.dk (P. Frigaard).

0378-3839/$ – see front matter © 2011 Elsevier B.V. All rights reserved.
doi:10.1016/j.coastaleng.2011.02.001

This paper presents physical model tests with combined waves and steady current while looking for a relationship between loading and initiation of motion. Based on the experiments, a correlation was found between the wave characteristics and initiation of motion for different current velocities. A linear relationship was derived between the critical bed shear-stress τ_{cr} and the bed shear-stress caused by current τ_c and waves τ_w leading to a design formula for a statically stable scour protection. This formula is hereafter referred to as the proposed design formula. In Section 2, the state of the art in scour protection design is summarized. Section 3 emphasizes on the experimental set-up, while Section 4 expands on the derivation of the proposed design formula, based on the results from the experiments. A significant reduction in required stone size for the scour protection is obtained when applying the proposed design formula. In a further approach, a more economical solution is aspired by using even smaller stone sizes for the scour protection and allowing limited stone motion for top layer stones. This method is dealt with in Part 2, following this paper (De Vos et al., in preparation).

2. State of the art in scour protection design

2.1. Need for scour protection

Before designing a scour protection, it is important to assess the influence of the scour hole on the design of a foundation, as this will determine whether the use of a scour protection is required. When the expected scour threatens the stability of the structure and/or the alternatives excessively raise costs, a scour protection is the way to go. Ballast Nedam and Oud (2002) and Herman et al. (2003) weigh the first alternative (scour development) against the application of a scour protection for a monopile foundation. This economical evaluation leads to the conclusion that in the examined case, the application of a scour protection leads to the most economic solution. However, the difference is limited so it is suggested to make further inquiries. In chapter 2 of De Vos (2008) all aspects of the influence of a scour hole on an offshore wind turbine are summarized and a typical example for an offshore wind turbine is calculated.

Furthermore, all failure mechanisms should be considered when designing a scour protection. Fig. 1 shows the relevant failure mechanisms for the scour protection around a monopile foundation (adapted from Hoffmans and Verheij (1997)). Comparable failure mechanisms are also listed by Chiew (1995) and Sumer and Fredsøe (2002):

a) erosion of the top layer caused by the flow, possibly leading to scour near the structure;
b) loss of subsoil through the scour protection, which may lead to sinking of the top layer in the bed. This can be an iterative process, eventually leading to scour holes near the construction;
c) due to the edge scour, which originates from the abrupt change in roughness between the riprap and the bed, stones may disappear at the edge of the scour protection, leading to an undersized scour protection (horizontal dimensions);
d) when the scour hole is to steep, flow slide may damage the scour protection from the edge.

In this paper, the main focus lies on the prevention of failure mechanism a) through the development of a design formula for the required stone size of the scour protection's top layer.

2.2. Existing design criteria

Several empirical criteria for the design of scour protections in a steady current (bridge piers) exist (Chiew, 1995; Hoffmans and Verheij, 1997; May et al., 2002), but the design of scour protections in a combined wave and current environment has only recently been dealt with by den Boon et al. (2004), Hansen and Gislason (2005), Grune et al. (2006) and Whitehouse et al. (2006). To the authors' knowledge, very few design methods were derived for a combined wave and current climate other than the method developed in the OPTI-PILE project from E-Connection et al. (2002–2004). A review of the OPTI-PILE project is therefore presented in this chapter. The scour protections of most offshore wind parks are designed based on the criteria of the threshold of motion (see below) followed by a physical model study (e.g. Kirkegaard et al., 1998). Most of these results are not reported in literature and therefore only a confined group of people has the knowledge and experience to design scour protections for offshore monopile foundations.

2.2.1. Design criteria based on the threshold of motion

The thesis of Shields (1936) is the best-known and most used in research on the threshold of motion in uniform flow. He defined the

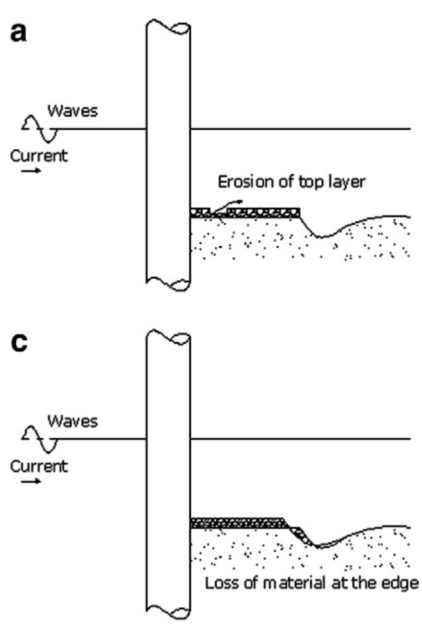

Fig. 1. Failure mechanisms for scour protection around an offshore monopile foundation; after Hoffmans and Verheij (1997).

parameter θ_{cr} for the threshold of motion as the Shields parameter at which particles are displaced by the flow:

$$\theta_{cr} = \frac{\tau_{cr}}{g(\rho_s - \rho_w)d_s} = \frac{u_{*cr}^2}{g\Delta d_s} \tag{1}$$

with τ_{cr} the threshold bed shear-stress, d_s the sediment grain diameter, g the gravitational acceleration, ρ_s and ρ_w respectively the density of sediment and water, u_{*cr} the critical shear velocity and $\Delta = (\rho_s - \rho_w)/\rho_w$.

When the critical Shields parameter is exceeded or in other words when the bed shear-stress exceeds the critical bed shear-stress, stones will be moved by the flow. For a steady, uniform flow U_c, the bed shear-stress τ_c is defined as:

$$\tau_c = \frac{1}{2}\rho_w f_c U_c^2 \tag{2}$$

with f_c a dimensionless friction coefficient of the bed. As τ_c is used in the derivation of the proposed design formula, the formula to calculate f_c (Liu, 2001) is given in Appendix A (Eq. (A.2)).

Several authors (Nielsen, 1992; Fredsøe and Deigaard, 1992; Soulsby, 1997) have adjusted Shields' formula to be applicable to the case of waves and combined waves and currents. In the case of waves, the bed shear-stress is oscillatory and has an amplitude τ_w which is obtained through the use of a wave friction factor f_w, equivalent to the friction coefficient f_c:

$$\tau_w = \frac{1}{2}\rho_w f_w U_m^2 \tag{3}$$

with U_m the amplitude of this horizontal velocity just above the bed and ρ_w the density of the water. In CIRIA/CUR (1991) it is described how both Grant and Komar and Miller have shown independently in 1975 that the results for initiation of motion for unsteady flow (waves) are in reasonable agreement with the Shields curve determined for steady flow (current) when the wave friction factor f_w, defined in Eq. (3), is used.

Several expressions for the wave friction factor f_w exist. The formulae which are most often used to calculate f_w are given in Appendix A. These formulae were compared when searching for the best design formula based on the experimental results.

In most marine environments, both currents and waves occur simultaneously. Difficulties arise because they interact and their combined influence is not the same as a linear sum of their separate influences. Several different theories and models have been proposed to calculate the bed shear-stress τ_{wc} in combined waves and current, leading to considerable differences in the predicted bed shear-stress. The work of Fredsøe and Deigaard (1992) and Soulsby (1997) is most often used to calculate the bed shear-stress in a combined wave and current climate. Their work is summarized in Appendix A.

The general design method for scour protections is to determine the amplified bed shear-stress near the pile and to use the Shields criterion as described above to establish the required stone size. The influence of a single vertical pile on the flow pattern in a steady current is well understood (Melville and Raudkivi, 1977; Hjorth, 1975; Baker, 1979; Dargahi, 1989; Sumer et al., 1997; Sumer and Fredsøe, 1997; Sumer and Fredsøe, 2002; among others) and several investigations exist on the flow pattern around a vertical pile in a wave field (Sumer and Fredsøe, 1997; Sumer and Fredsøe, 2002). Limited information however is available on the flow pattern in a combined wave and current case (Umeda et al., 2003; Sumer et al., 1997).

When a vertical pile is placed on a sea bed, the changes in the flow pattern generally create an increase in the bed shear-stress and in the turbulence level near the structure, both leading to an increase in local sediment transport capacity near the structure. The increase in the bed shear-stress is traditionally expressed in terms of a so-called amplification factor α, which is defined by

$$\alpha = \frac{\tau_b}{\tau_{b,\infty}} \tag{4}$$

in which τ_b and $\tau_{b,\infty}$ represent the actual and the undisturbed bed shear-stress, respectively.

Most authors (Breusers and Raudkivi, 1991; Hoffmans and Verheij, 1997; Van Oord, 2003) state that the threshold of motion around a cylindrical vertical pile is reached when the amplified bed shear-stress, equal to 4 times the undisturbed bed shear-stress exceeds the critical bed shear-stress τ_c ($\alpha = 4$). Or, when turning things around, in order to guarantee a stable scour protection, the following criterion needs to be fulfilled:

$$\tau_{cr} > 4\tau_{b,\infty} \text{ or } U_{cr} > 2U_c. \tag{5}$$

For sufficiently coarse bed material, the critical Shields parameter reaches a constant value of 0.056 (Shields, 1936). For most scour protections, this constant value is withheld as the threshold value. However, Hoffmans and Verheij (1997) note that, because of the non-uniform distribution of the mixtures, Shields drew not a single curve, but a broad belt. They present a variation on the Shields curve, shown in Fig. 2. They plot the Shields parameter versus the dimensionless grain size D_*, defined as:

$$D_* = \left[\frac{g(s-1)}{\nu^2}\right]^{1/3} d_s \tag{6}$$

with d_s the sediment grain diameter, ν the kinematic viscosity of water and s the relative density of the stones $= \rho_s/\rho_w$.

Fig. 2 shows that the Shields criterion actually corresponds with the initiation of motion over the entire bed. Occasional particle movement may occur at some locations for much smaller values of the Shields parameter. Therefore, a smaller value for the critical Shields parameter is used to derive the proposed design formula. This is also in agreement with CIRIA/CUR (1991), which recommends adopting a smaller critical Shields parameter when a time-averaged shear stress is used.

A comparable but somewhat different design approach is suggested by Whitehouse (1998), who discusses scour protections in a marine environment (both waves and currents). He mentions that the calculation of the bottom shear-stress is complicated due to the fact that the shear-stress acting on the protection layer is determined by the characteristics of the protection material, which are not known a priori. He suggests getting an initial estimate of the material that will be stable under the design current or wave action by implementing

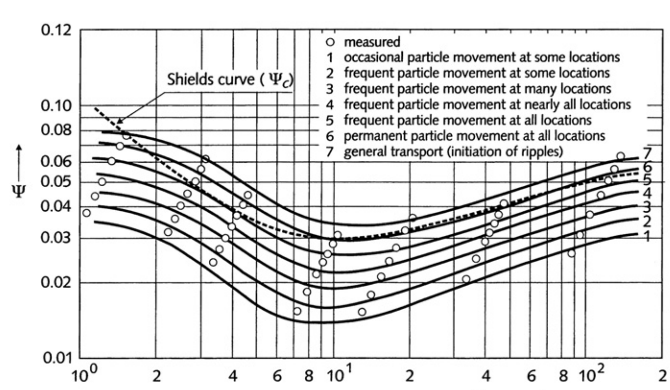

Fig. 2. Modified Shields diagram plotting the Shields parameter ψ as a function of dimensionless grain size D_*; Hoffmans and Verheij (1997).

Eqs. (7) and (8), suggested by Soulsby (1997) for an undisturbed bed. An iterative approach, based on the calculation of the bed shear-stress can then be used to refine these estimates. The initial estimate for the critical stone diameter D_{cr} for a steady current is (according to Soulsby (1997)):

$$D_{cr} = \frac{0.25U_c^{2.8}}{d^{0.4}[g(s-1)]^{1.4}} \text{ for stone diameters} > 10\,\text{mm} \tag{7}$$

with U_c the amplified steady flow velocity, d the water depth, g the gravitational acceleration and s the relative density of the stones. For a steady flow, the amplification of the steady flow can be assumed to be 2 times the average steady flow velocity.

For waves the initial estimate for the critical stone diameter D_{cr} is:

$$D_{cr} = \frac{97.9U_m^{3.08}}{T_p^{1.08}[g(s-1)]^{2.08}} \text{ for stone diameters} > 10\,\text{mm} \tag{8}$$

with U_m the amplified amplitude of the horizontal wave induced orbital velocity above the bed, calculated according to the method described in Soulsby (1997), T_p the peak wave period, g the gravitational acceleration and s the relative density of the stones. For the amplification of the bed shear stress in case of waves, Soulsby suggests a value $\alpha = 2.2$, this implies an amplification of the orbital velocity of $\sqrt{2.2}$.

However Whitehouse (1998) does not propose which scour protection strategy is appropriate for the combined wave and current situation.

There are several disadvantages to the methods described above to calculate the required stone size of a scour protection. First of all, there exists a variety of possibilities to calculate the wave-induced bed shear-stress. Secondly, the hydraulic roughness of the sand bed is smaller than that of the scour protection. This sudden increase in roughness gives rise to another non-uniform flow, characteristic for bed protections (Hofland, 2005; Whitehouse, 1998). This effect is not taken into consideration when calculating the bed shear-stress at the scour protection. Furthermore, different amplifications due to the presence of the pile are measured for waves and currents; Van Oord (2003) mentions that the amplification of the bed shear-stress due to the presence of the pile is limited to 2.25 for waves with a KC number smaller than 6, whereas it is 4 for a steady current. Sumer and Fredsøe (2002) mention much higher values for the amplification in a steady current. The combined wave and current bed shear-stress on the other hand is not a linear composition of the separate bed shear-stress for waves and current. It is difficult to give a theoretical estimate of the combined effect of these two phenomena on the final amplified bed shear-stress.

2.2.2. Design criterion based on the OPTI-PILE study

The OPTI-PILE project was funded by the European Commission (Fifth Research and Technological Development Framework Programme) and ran for two years from early 2002. It was co-ordinated by E-Connection Project BV, P.O. Box 101, 3980 CC Netherlands. Other partners were Vestas - Wind Systems (DK) and Germanischer Lloyd Windenergie (D).

The goal of the project was to optimize monopile foundations for offshore wind turbines in deep water and for North Sea conditions. OPTI-PILE was part of the engineering of the 120 MW Offshore wind park Q7-WP located 23 km off the Dutch coast at IJmuiden in water with a depth varying from 20 to 25 m. The results of the Q7 project are generalized towards other similar locations and the OPTI-PILE project is thus of relevance for many offshore areas with similar characteristics.

One part of the OPTI-PILE project aimed to improve the design for scour protections in combined waves and current. A physical model study was performed on scale 1/47.25 at HR Wallingford, testing the following conditions (den Boon et al., 2004):

- scour depth for an unprotected monopile foundation;
- damage to scour protection designs (supplied by van Oord ACZ).

Froude scaling was applied. Two types of scour protections were tested, a so-called static protection, which is designed according to the theory described above, and a dynamic protection. For the dynamic protection, a scour hole was allowed to develop and was then backfilled with scour protection material (comparable to the scour protection design for the Scroby Sands wind farm, described by Cefas (2006) and Hansen and Gislason (2005)).

The test conditions are described in Table 1, which gives both prototype and model scale dimensions. The tests ran for one model hour and damage was determined using radial bed profiles, measured with a touch-sensitive bed profiler, and overhead photographs.

The results from the tests were:

- in the situation without scour protection, a scour hole of up to 1.75 times the pile diameter D developed;
- both the static and the dynamic scour protections prevented erosion around the monopile;
- significantly smaller rock sizes could be used for the dynamic protection;
- a stability parameter *Stab* is able to describe the damage state of the scour protection.

In the OPTI-PILE project the tests were classified into three damage categories for the scour protection:

- no movement of rocks;
- some movement, but no failure;
- failure.

The scour protection is considered to have failed when the filter layer is exposed over a minimum area of four armor units ($4D_{50}^2$) or, when no filter is present (in the dynamic scour protections) when a

Table 1
Test conditions for the OPTI-PILE project.

Parameter	Symbol	Unit	Tested range (prototype)	Tested range (model scale)
Significant wave height	H_{m0}	[m]	6.5–8.5	0.138–0.180
Mean wave period	T_m	[s]	8.9–9.6	1.3–1.4
Current velocity in combined wave and current situation	U_c	[m/s]	1.01–1.15	0.147–0.170
Current velocity in current alone situation	U_c	[m/s]	2.01–2.06	0.295–3.03
Water depth	D	[m]	24	0.508
Extension of the scour protection	L_s	[m]	15; 25; 35	0.32–0.53–0.74
Pile diameter	D	[m]	4.2	0.89
Median stone diameter for static protection	D_{50}	[m]	0.607; 0.396; 0.222	0.0115; 0.0075; 0.0042
Thickness of armor layer for static protection		[–]	$3D_{n50}$	$3D_{n50}$
Thickness of filter layer for static protection		[m]	0.5	0.01
Median stone diameter for dynamic protection	D_{50}	[m]	0.591; 0.396; 0.222; 0.121	0.0112; 0.0075; 0.0042; 0.0023
In-fill height of dynamic scour protection		[–]	1/3; 2/3; fully filled	1/3; 2/3; fully filled

volume of rock has disappeared equal to the volume of rock required to cause failure for a scour protection with filter.

The stability parameter *Stab* is defined as:

$$Stab = \frac{\theta_{max}}{\theta_{cr}} \tag{9}$$

with θ_{cr} the critical Shields parameter = 0.056 and θ_{max} the maximum Shields parameter, defined as:

$$\theta_{max} = \frac{\tau_{max}}{\rho_w g(s-1)D_{50}} \tag{10}$$

and τ_{max} defined as in Eq. (A.21).

The value of the stability parameter *Stab* is plotted against the damage categories (Fig. 3) and two limits are found for the stability parameter, $Stab_{1,2}$ and $Stab_{2,3}$, which define the transition between the damage categories. For the tested range, their values are:

$$\begin{aligned} Stab_{1,2} &= 0.415 \\ Stab_{2,3} &= 0.460. \end{aligned} \tag{11}$$

When assuming that the critical Shields parameter represents initiation of motion, Eq. (11) implies that due to the presence of the pile, an amplification factor of 2.4 has to be taken into account.

In den Boon et al. (2004), the results are compared against two prototype wind farms, Horns Rev and Scroby Sands. The conclusion is that a smaller stone size could have been applied for Horns Rev, whereas some damage to the Scroby Sands scour protection is expected. The latter was however designed as a non-maintenance free scour protection.

den Boon et al. (2004) comment that the choice of friction factor f_w significantly affects the value of θ_{max} and thus the interpretation of the results. However, the friction factor they apply only gives a weak dependence of θ_{max} on the stone size D_{50}, which implies that the boundaries of stability can be less clear. They note that friction factor tuning is possible with experimental model tests, but has yet to be investigated.

In Whitehouse et al. (2006) another test series is described for which the OPTI-PILE stability was verified. The test series was carried out for the Arklow Bank Wind Park, which is subject to strong currents and high waves. Tests were performed on scale 1/36. In this project, larger rock sizes are applied, due to the high loads and damage is defined as the number of stones which are displaced by more than one diameter and subsequently calculate the damage for each quadrant. For smaller rock gradings, damage was assessed using bed profiling. When applying the OPTI-PILE stability parameter, Whitehouse et al. (2006) conclude that the stability parameter *Stab* is not closely related to the maximum damage and would need to be recalibrated for the specific circumstances of the Arklow Bank offshore wind park.

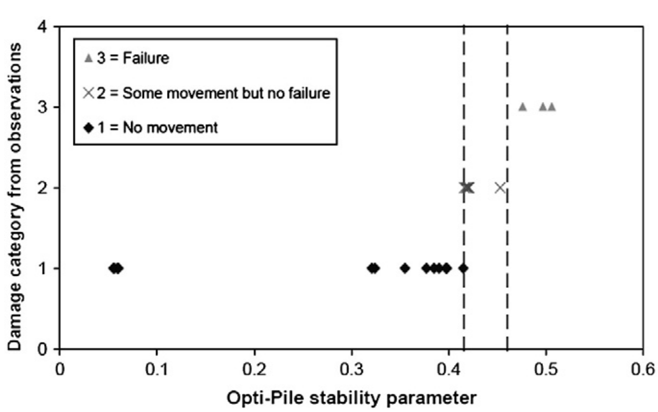

Fig. 3. Damage categories against stability parameter (OPTI-PILE project); from den Boon et al. (2004).

3. Experimental set-up

3.1. General description of set-up and model

All experiments are conducted at the department of Civil Engineering of Ghent University. Fig. 4 shows a sketch of the set-up in the wave flume. The dimensions of the flume are 30 m in length, 1 m in width and 1.2 m in height. One of the flumes' side walls is partially made of glass to facilitate visual observations. A piston type wave paddle is used to generate waves, suitable for shallow water wave generation. An exterior pump-circuit can generate currents in both directions, permitting a current following or opposing the waves.

Part of the floor was lifted to create a movable bed in the middle of the flume and the transition from the bottom of the flume to the sand bed was made with a gentle slope of 1/20. Very fine, uniform sand with a diameter of 100 μm was used for the movable bed to minimize scale effects. A model of a monopile is built in the middle of the wave flume, centrally in the 4 m long sandbox. The monopile was placed centrally between the two current inlets to minimize the differences in the flow pattern when the current is reversed. The length of the sandbox is chosen large enough to avoid influence of edge effects on the results (as there is no feeding of the sediment, edge effects may exist at the edges of the sandbox). The height of the sandbox (0.3 m) is chosen large enough for any expected scour to develop without any influence of the fixed bottom.

A spending beach with slope 1/5 was installed at the end of the flume, to reduce reflections. The gravel beach developed its own profile, reducing reflection till less than 15%.

The diameter of the monopile is 0.1 m and represents a typical monopile foundation for offshore wind turbines in the North Sea on a scale 1/50. Froude scaling is applied. A scour protection made of stones is placed around the monopile foundation, placed on top of a geotextile filter. Stones are painted in different colors to allow visual observation of the amount and direction of displacement. The colored stones are placed in concentric circles around the pile, as shown in Fig. 5 and each ring has a width equal to the piles' radius. The diameter of the applied scour protection is 5 times the pile diameter. 10% extra material is used for the outer ring, to make sure some material is placed beside the geotextile without decreasing the height of the outer ring. The thickness of the scour protection layer is $2.5D_{n50}$.

A geotextile filter was installed on top of the sand. Fig. 6 shows the construction sequence of the scour protection. The concentric circles are placed one after the other and were flattened by hand to obtain a leveled scour protection. The construction was done under water.

Although it is sometimes advised to place the top of the scour protection at the same level of the surrounding bed (Melville and Coleman, 2000), this is not done here for several reasons. Firstly, the scour protection is placed above the seabed because Ballast Nedam and Oud (2002) showed that this is the most economical solution (compared to dredging and leveling the scour protection with the bed). The second reason is that the increase in wave load due to the higher location of the scour protection is very limited. The influence is mainly restricted to edge effects, which are disregarded here. Finally, when the scour protection is placed level with the sea bed, a global lowering of the sea bed due to overall sand transport will cause the same situation as described above. When large variations of the seabed are expected, a scour protection placed in a fully developed scour hole as applied at the Scroby Sands wind farm might offer a better solution (Hansen and Gislason, 2005; Cefas, 2006).

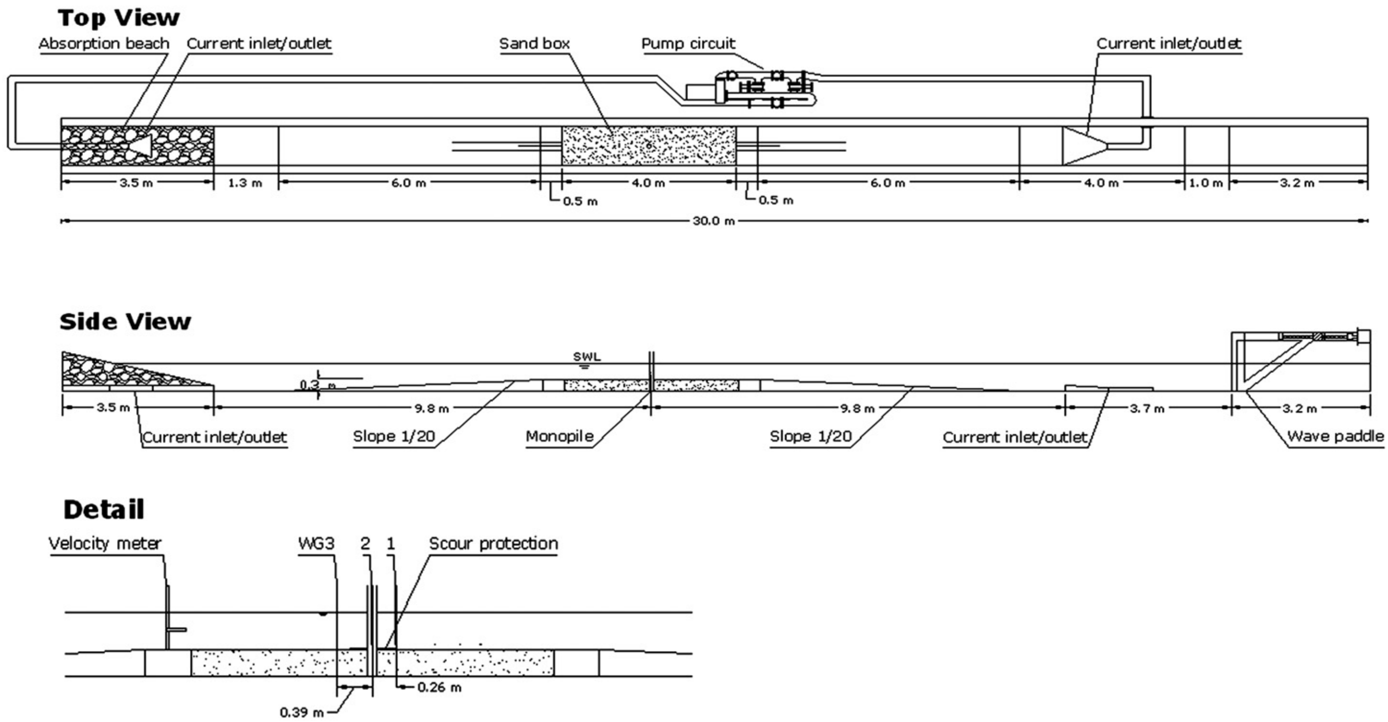

Fig. 4. Experimental set-up in the wave flume.

3.2. Hydraulic conditions

Consecutive tests were carried out with increasing current velocities (target velocities of 0 m/s to 0.28 m/s, in steps of 0.07 m/s). Regular waves were superimposed on the current: for a given wave period and current velocity, wave height was increased in small steps until movement initiated. For a given steady current velocity, the test was performed with different wave periods. The complete test program is given in Table 2. In Table 2, the wave heights required to initiate movement are given. Initiation of movement is visually observed and is regarded as the displacement of at least one stone over a distance of at least two times the median stone size D_{50}.

Several tests were carried out after one another. It is possible that, just after installation of a scour protection, some stones are displaced almost immediately due to an unstable position (Hofland, 2005). To avoid underestimation of the wave height that initiates movement due to this "water working", tests which were carried out on a newly placed scour protection were repeated at the end of the test series.

The records of regular waves contain approximately 50 waves. Very small variations in the wave height occur, due to a small reflection at the end of the wave flume. The wave height used for the analysis is the maximum wave height, measured at the location of the pile and determined using the zero down-crossing method. The current velocity U_c is measured at a height of approximately 0.4d above the flat concrete bed behind the pile (Fig. 4).

Table 2 also gives the values of τ_c, τ_w and $\tau_c/(\tau_c+\tau_w)$. The ratio $\tau_c/(\tau_c+\tau_w)$ gives an indication of the wave-current regime (Malarkey and Davis, 1998). When $\tau_c/(\tau_c+\tau_w)=0$, the tests are wave dominated, and when $\tau_c/(\tau_c+\tau_w)=1$, the test is current dominated. For the present tests, the regime varies between the wave-dominated regime ($\tau_c/(\tau_c+\tau_w)=0$) and the wave-current interaction regime ($\tau_c/(\tau_c+\tau_w)=0.78$).

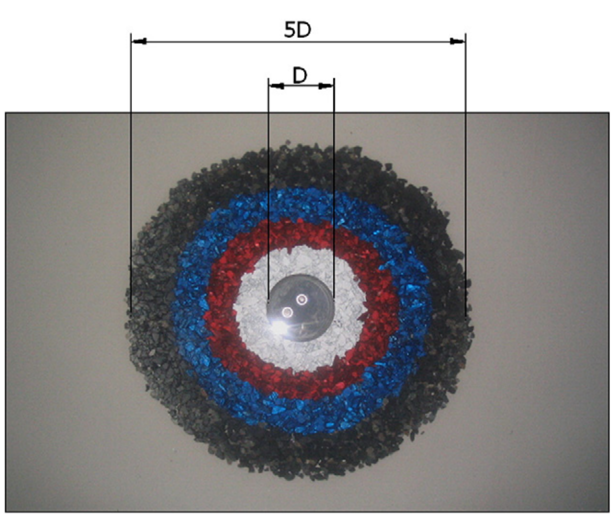

Fig. 5. Top view of a scour protection, before loading (note that the pile was removed for making measurements and for taking pictures).

3.3. Scour protection characteristics

Three different rock armor gradings are used throughout the tests. The gradings which were used are: 2–80 kg, 2–300 kg and 80–300 kg (prototype values). The resulting median grain sizes in model scale are D_{50} are 4.1 mm, 6.0 mm and 8.5 mm, leading to a nominal stone size D_{n50} of 3.4 mm, 5.0 mm and 7.1 mm ($D_{n50}/D_{50}=0.84$). The gradings and their respective standard grading limits are shown in Fig. 7. The full line represents the target gradings which were used, while the dotted line represents the measured grading. Target and measured grading coincide almost perfectly, as the gradings were obtained by carefully mixing amounts of sieved stones. The value of D_{85}/D_{15}, which represents the grading width according to CIRIA/CUR (1991) is shown in Table 3, together with the other scour protection characteristics.

The stones of the scour protection existed of angular rocks with a mass density $\rho_s=2650$ kg/m^3. The bulk density of the stones was

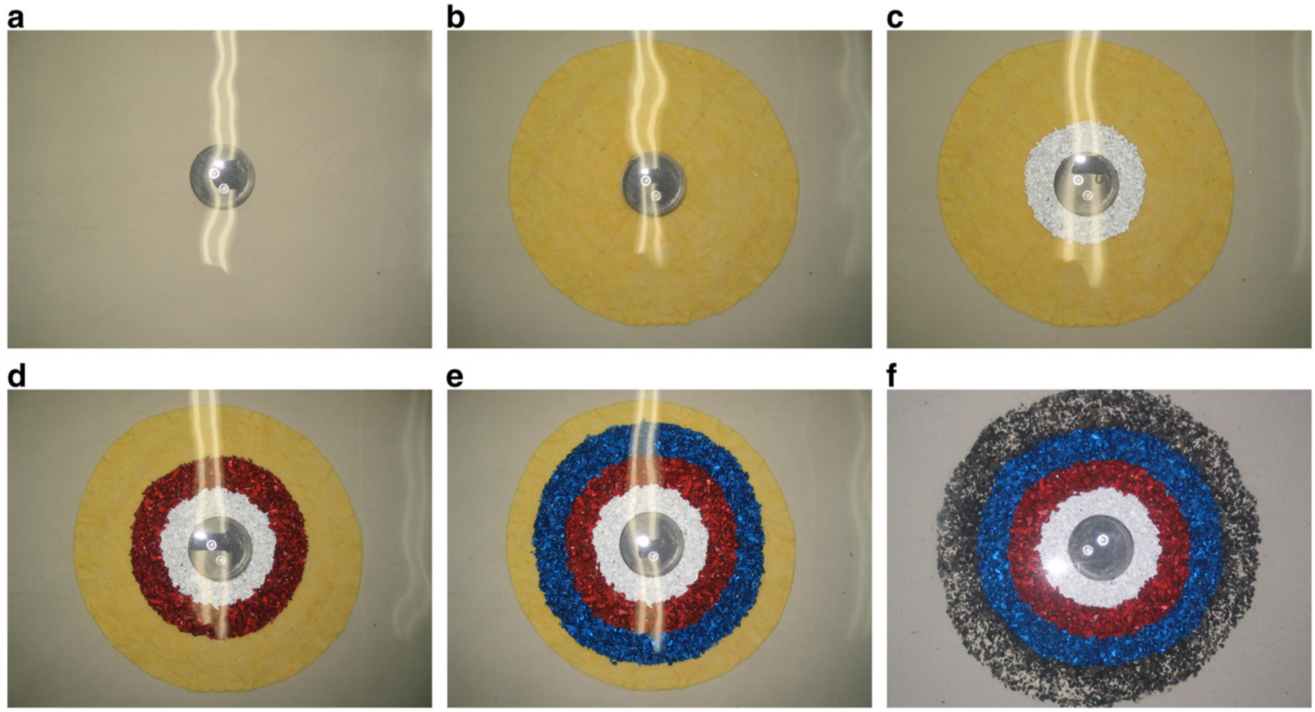

Fig. 6. Construction of the scour protection: (a) leveled sand bed; (b) placement of the filter; (c), (d), (e) and (f): consecutive placement of the top layer in concentric circles.

Table 2
Experimental conditions for static stability tests.

Test no. [–]	d [m]	D_{n50} [mm]	U_c [m/s]	T_w [s]	H [m]	τ_c [N/m^2]	τ_w [N/m^2]	$\tau_c/\tau_c+\tau_w$ [–]
1	0.4	3.45	0.000	1.13	>0.120	0.00	1.94	0.00
2	0.4	3.45	0.000	1.41	0.105	0.00	1.84	0.00
3	0.4	3.45	0.000	1.7	0.099	0.00	1.68	0.00
4	0.4	3.45	0.072	1.41	0.111	0.02	1.96	0.01
5	0.4	3.45	0.072	1.7	0.099	0.02	1.68	0.01
6	0.4	3.45	0.160	1.41	0.106	0.11	1.85	0.06
7	0.4	3.45	0.160	1.7	0.097	0.11	1.63	0.06
8	0.4	3.45	0.220	1.13	0.074	0.21	1.10	0.16
9	0.4	3.45	0.220	1.41	0.044	0.21	0.64	0.25
10	0.4	3.45	0.220	1.7	0.033	0.21	0.45	0.32
11	0.2	3.45	0.302	1.41	0.011	0.51	0.22	0.70
12	0.2	3.45	0.302	1.7	0.008	0.51	0.14	0.78
13	0.4	3.45	−0.067	1.41	0.112	0.02	1.98	0.01
14	0.4	3.45	−0.067	1.7	0.093	0.02	1.56	0.01
15	0.4	3.45	−0.142	1.41	0.099	0.09	1.71	0.05
16	0.4	3.45	−0.142	1.7	0.072	0.09	1.15	0.07
17	0.4	5.00	0.000	1.41	0.159	0.00	4.09	0.00
18	0.4	5.00	0.000	1.7	0.129	0.00	3.12	0.00
19	0.4	5.00	0.076	1.41	0.132	0.03	3.27	0.01
20	0.4	5.00	0.076	1.7	0.130	0.03	3.16	0.01
21	0.4	5.00	0.158	1.41	0.136	0.12	3.40	0.03
22	0.4	5.00	0.158	1.7	0.135	0.12	3.29	0.04
23	0.4	5.00	0.228	1.41	0.124	0.26	3.03	0.08
24	0.4	5.00	0.228	1.7	0.075	0.26	1.65	0.14
25	0.2	5.00	0.300	1.41	0.025	0.58	0.84	0.41
26	0.2	5.00	0.300	1.7	0.030	0.58	0.94	0.38
27	0.4	5.00	−0.137	1.41	0.134	0.09	3.34	0.03
28	0.4	5.00	−0.137	1.7	0.127	0.09	3.06	0.03
29	0.4	7.14	0.000	1.41	0.151	0.00	5.09	0.00
30	0.4	7.14	0.000	1.7	0.133	0.00	4.29	0.00
31	0.4	7.14	0.074	1.41	0.152	0.03	5.12	0.01
32	0.4	7.14	0.074	1.7	0.162	0.03	5.44	0.01
33	0.4	7.14	0.148	1.41	0.120	0.12	3.86	0.03
34	0.4	7.14	0.148	1.7	0.125	0.12	3.97	0.03
35	0.4	7.14	0.223	1.41	0.104	0.28	3.24	0.08
36	0.4	7.14	0.223	1.7	0.093	0.28	2.78	0.09
37	0.2	7.14	0.297	1.41	0.030	0.66	1.34	0.33
38	0.2	7.14	0.297	1.7	0.030	0.66	1.24	0.34
39	0.4	7.14	−0.134	1.41	0.118	0.10	3.76	0.03
40	0.4	7.14	−0.134	1.7	0.128	0.10	4.11	0.02

found to lie in between 1.45 and 1.5. To calculate the required weight of stones, a porosity of 40% was assumed.

Washing out of fine bed material through the rocks might cause failure of the scour protection. This is avoided by applying a filter layer between the bed and the scour protection's top layer. For offshore situations it is common to use a granular filter (1 or 2 layers). However, during the tests a geotextile was used as a filter for the sake of convenience and because the main interest of the experiments is the stability of the scour protection layer.

4. Analysis of the experimental model tests

As mentioned above, most scour protections are designed according to a static stability criterion, which states that stones have to remain stable under the maximum load. The presented test series is performed to assess which formula could lead to a more economical design, while still pursuing static stability (no movement). In order to do this, combined regular wave and current tests were performed to obtain the load at which movement initiates.

4.1. Analysis method

The measured wave height and wave period are used to calculate the amplitude of the orbital velocity near the bed (using linear wave theory):

$$U_m = \frac{H}{2}\frac{gT_w}{L}\frac{1}{\cosh\left(\frac{2\pi d}{L}\right)} \tag{12}$$

with H the wave height, g the gravitational acceleration, T_w the wave period, L the wave length and d the water depth.

At first, a direct relation was sought between stone size and flow velocity (both wave and current), as suggested by Breusers and Raudkivi (1991), May et al. (2002) and Chiew (1995), which all in some way suggest a relationship between critical stone size and U^2 or U^3. No adequate direct relationship was found between these parameters and regression analysis was used to find a better solution.

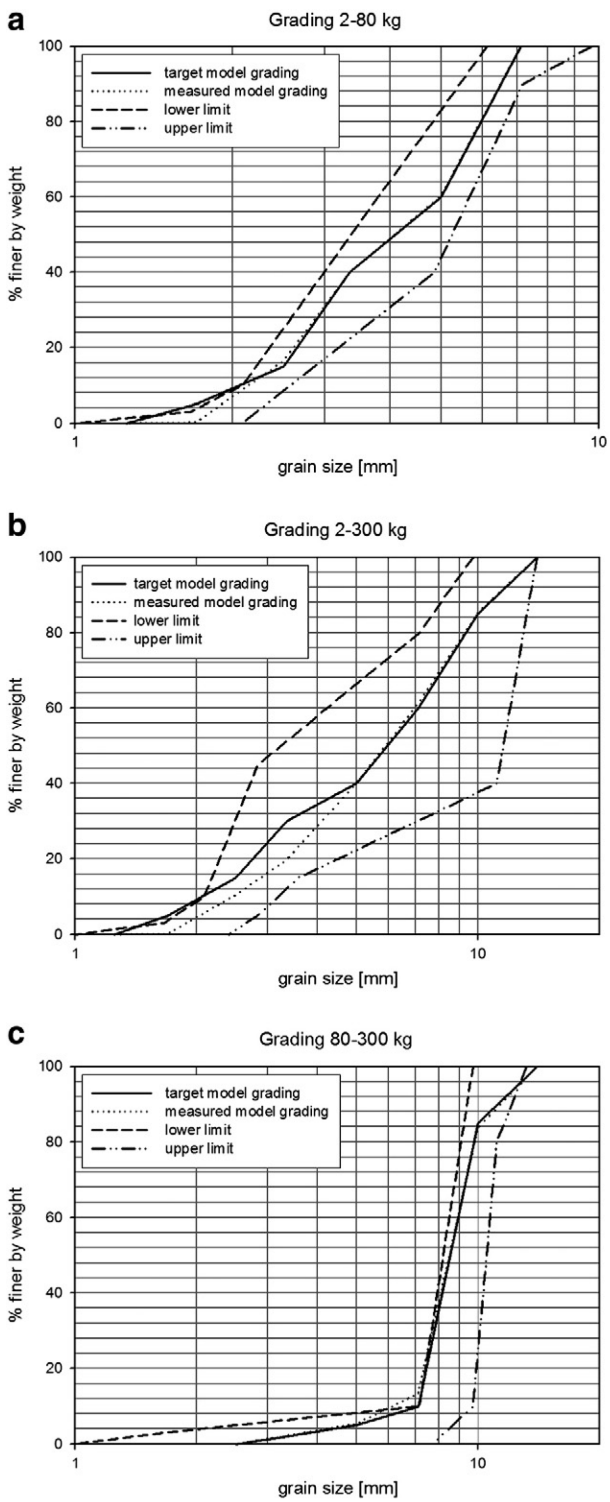

Fig. 7. Tested rock gradings (grain sizes in model scale): (a) 2–80 kg; (b) 2–300 kg; (c) 80–300 kg (prototype scale).

The orbital velocity (Eq. (12)) and the measured current velocity are used to calculate the undisturbed bed shear-stresses near the bed. Undisturbed implies that we assume no pile is present. The equations used to calculate the bed shear-stress are found in Appendix A. Eqs. (A.1), (A.2) and (A.3) are used to calculate the bed shear-stress, caused by a current. To calculate the wave induced bed shear-stress (Eq. (A.6)), several methods to determine f_w are compared: Eq. (A.8) (Fredsøe and Deigaard, 1992); Eq. (A.12) (Dixen et al., 2008); Eq. (A.14) (Nielsen, 1992) and Eq. (A.15) (Soulsby, 1997). Several

Table 3
Scour protection characteristics.

Prototype grading	Model value of D_{50} [mm]	Model value of D_{n50} [mm]	D_{85}/D_{15} [–]	$D_{67.5}$ [mm]
2–80 kg	4.1	3.4	2.48	5.4
2–300 kg	6.0	5.0	4.00	7.9
80–300 kg	8.5	7.1	1.39	9.1

linear and non-linear relations were explored between the value of the critical bed shear-stress τ_{cr} and the undisturbed bed shear-stress caused by the steady current and the waves. Also the mean combined bed shear-stress τ_m and the maximum combined bed shear-stress τ_{max} were included in the analysis.

The critical Shields parameter for initiation of movement is assumed to be a constant value = 0.035, as even for the smallest tested stone size, the dimensionless grain size D^* is sufficiently large (larger than 100).

The wave height which initiates movement for the different combinations of U_c, T_w and D_{50} is shown in Table 2. Before performing the regression analysis, the differences between the alternative formulae to calculate the wave related bed shear-stress are demonstrated in Figs. 8 and 9. The values of T_w and D_{50} which were tested are marked in the figures.

As can be seen in Fig. 8 Eq. (A.14), suggested by Nielsen (1992) results in unexpected values of the wave induced bed shear-stress for small values of the wave period. It is therefore advised to be careful when using this equation. It is in any case advised to restrict the use of the regression formulae, suggested below, to the region of the tested parameters.

The best result for the regression analysis was obtained by using a combination of τ_c, determined according to Liu (2001) (Eqs. (A.1), (A.2) and (A.3)) and τ_w, calculated with Dixen et al. (2008) (Eqs. (A.6) and (A.12)) to estimate the critical bed shear-stress related to the threshold of motion. From now on, these equations are used to calculate the bed shear stress caused by the current and the waves. As is shown in Figs. 8 and 9, a different result will be obtained when using another equation. An example on how to interpret the results is presented in Figs. 10 and 11.

In an undisturbed condition, where the scour protection is covering the entire bed and the flow is not disturbed by a structure (Fig. 11(a)), the expectation is that movement is initiated when the bed shear-stress equals the critical bed shear-stress. The Shields criterion is used to determine the critical bed shear-stress. When the loading exceeds the resistance, stones will be moved by the flow. Whenever the resistance is larger than the load, the stones will stay in

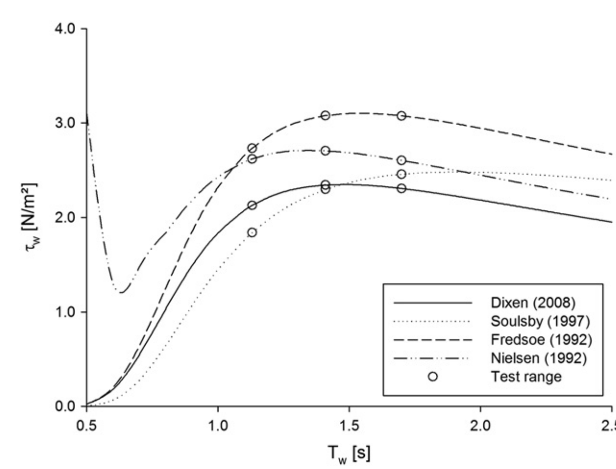

Fig. 8. Wave related bed shear-stress τ_w as a function of wave period T_w: $d = 0.4$ m; $H = 0.1$ m; $D_{50} = 6$ mm.

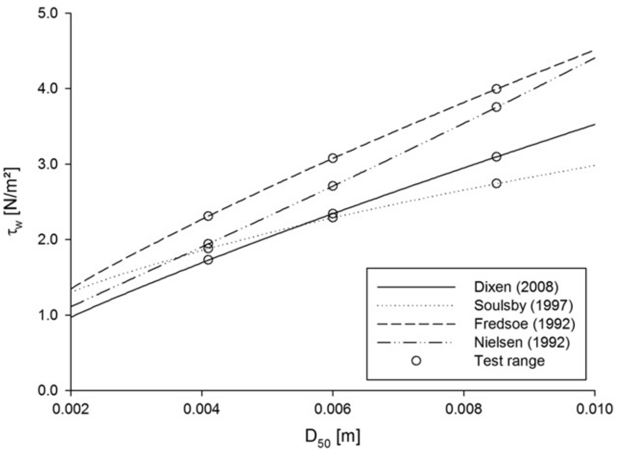

Fig. 9. Wave related bed shear-stress τ_w as a function of stone size D_{50}: $d=0.4$ m; $H=0.1$ m; $T_w=1.4$ s.

place. In the case a pile is present (Fig. 11(b)), the disturbance of the flow will cause the stones to move at a lower undisturbed load than would be expected in situation (a). An example of a regression fit on the measured data points (average value and 95% prediction interval) is shown in Fig. 10. As it is more intuitive, the example uses only 1 predictor variable.

Fig. 10 shows that for a value of the critical bed shear-stress $\tau_{cr,ex}$, the following situations occur for increasing bed load:

- τ_A: the critical bed shear-stress is large enough to avoid motion of the stones
- τ_B: motion is initiated in the case a pile is present. The undisturbed load τ_B is however smaller than the load τ_C at which movement is initiated without presence of the pile
- τ_C: initiation of motion takes place in the undisturbed case. In case a pile is present, several stones will already be displaced
- τ_D: movement of stones takes place both with and without pile.

4.2. Derivation of design formula for statically stable scour protection around monopile foundations based on experimental results

A regression analysis is performed to determine whether the load which initiates movement can be estimated from the present data set. The loading conditions (τ_c and τ_w) for each test are calculated in

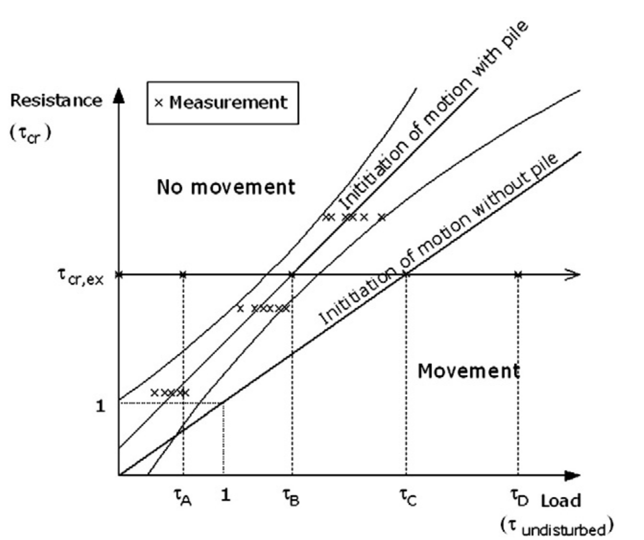

Fig. 10. Relation between undisturbed bed shear-stress τ (load) and critical bed shear-stress τ_{cr} (resistance).

undisturbed conditions. The value of the wave friction factor was calculated according to the formula of Fredsoe and Deigaard (1992), Soulsby (1997) and Dixen et al. (2008) as explained in Section 4.1. The best result was obtained when regressing τ_w determined according to Dixen et al. (2008) (Eqs. (A.6) and (A.12)), and τ_c (Eqs. (A.1), (A.2) and (A.3)) against τ_{cr}. The regression analysis led to the following formula:

$$\tau_{cr,pred} = 1.659 + 3.569\tau_c + 0.765\tau_w. \tag{13}$$

The r^2 value, representing the coefficient of determination, equals 0.90 for Eq. (13).

The predicted value $\tau_{cr,pred}$ is plotted against the measured value $\tau_{cr,meas}$ in Fig. 12. As each target rock grading was obtained by carefully mixing grains with different sizes, the same value of $\tau_{cr,meas}$ was obtained during the model tests for all tests with the same value of D_{50}.

The value of $\tau_{cr,}$ is determined by assuming $\theta_{cr}=0.035$ and a value $D_{67.5}$ instead of D_{50} to calculate the critical bed shear-stress τ_{cr} for the scour protection:

$$\theta_{cr} = 0.035 = \frac{\tau_{cr}}{\rho_w g(s-1)D_{67.5}}. \tag{14}$$

With s the relative density of the stones (ρ_s/ρ_w); g the gravitational acceleration and ρ_w the density of water.

The value of $D_{67.5}$ is used instead of D_{50} to calculate τ_{cr}, as the results showed that stones in a scour protection with a smaller grading tend to move faster than those in a scour protection with a wide grading. The reason why scour protections with a wide grading appear to be more stable is probably due to the fact that in widely graded material, smaller stones find a better shelter thanks to the larger stones. A possibility to account for this, is to calculate the value of τ_{cr} with a larger stone size in the stone grading (e.g. $D_{67.5}$). This way, the value of τ_{cr} will be significantly larger for the same value of D_{50} for a wide grading, compared to a narrow grading.

It is important to note that $2.5D_{50}$ is used for the bottom roughness k_s to calculate the bed shear-stresses caused by waves and current in Eq. (13), so both values of D_{50} and $D_{67.5}$ are required to calculate the required stones size.

It is important to stress that Eq. (13) is not a dimensionless equation. In Eq. (13) τ_c, τ_w and $\tau_{cr,pred}$ are calculated assuming a length scale of 1/50. This means that, when scaling to a scale 1/1, Eq. (13) changes into:

$$\tau_{cr,pred} = 83 + 3.569\tau_c + 0.765\tau_w \tag{15}$$

in which the values for the bed shear stress are expressed in N/m^2. Eq. (15) should therefore be used to calculate the required bed shear stress in prototype scale.

Section 4.4 recapitulates how to use Eq. (15) to calculate the required stone size for a statically stable armor layer.

4.3. Adjustment of the design formula for irregular waves

Eq. (15) is derived based on results of regular wave tests. This implies that the same load is experienced near the scour protection every time a wave passes. In reality however, a sea state consists of irregular waves with varying wave height and period, leading to varying loads on the scour protection material.

Two design approaches can be used to determine the initiation of stone entrainment in irregular wave conditions based on the results from the regular wave tests: a probabilistic or a deterministic approach (CIRIA/CUR, 1991). With a probabilistic approach the probability of stone entrainment is assessed by taking the probability distribution of both the load (wave and current characteristics) and the stone entrainment which belongs to each particular load into account. A deterministic approach on the other hand uses a

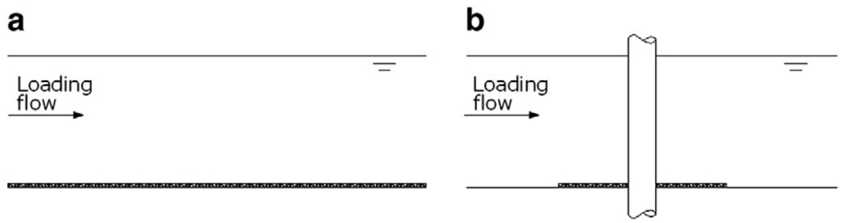

Fig. 11. Bed protection without (left) and with (right) presence of a pile.

characteristic value of the loading and a characteristic strength value to determine whether stone entrainment will take place.

We opt for the use of the traditional design method, the deterministic approach, which allows for a simple calculation of the required stone size. Thus a representative value for the irregular wave load in Eq. (15) needs to be found. The wave load on the seabed can be represented by the bottom shear-stress, which is mainly influenced by the orbital bottom velocity. The larger bottom velocities in a wave train are more likely to cause the stones to move. The question is which value of the bottom velocity will best represent the wave shear-stress and how this value can be retrieved from the spectrum.

The irregular wave test results which are used to assess which value of the bottom velocity is best used to calculate the wave induced bed shear-stress in Eq. (15) are described in "Empirical design of scour protections around monopile foundations. Part 2: Including damage number in the stability criterion" by De Vos et al. (in preparation). It appears that a good result is obtained by using $H_{1/10}$ (average of 10% highest waves) and T_p to calculate U_m according to Eq. (12). When the waves are Rayleigh distributed, the value of $H_{1/10}$ can be calculated as (CEM, 2002):

$$H_{1/10} = 1.27H_s. \tag{16}$$

Eq. (15) can thus be used to assess the required stone size for a scour protection around a monopile foundation when using $H_{1/10}$ and T_p to calculate U_m and A ((Eqs. (12) and (A.10)) and Eq. (A.6) to calculate τ_w.

4.4. Implementation of the design formula

Eq. (15) can be used to verify whether a given scour protection is statically stable or to design a new scour protection. In the latter case, an iterative process is necessary to calculate the required armor layer stone size, for which static stability (i.e. no movement of top stones) is guaranteed during a design storm, as both the load and the resistance of the top layer are depending on the stone size. Fig. 15 illustrates the procedure which can be followed in this case.

The required input data are:

- water depth: d
- design depth-averaged flow velocity: U_c
- design wave conditions: significant wave height H_{m0} and peak wave period T_p
- rock density: ρ_s
- water density: ρ_w
- rock grading: D_{85}/D_{15}
- initial estimate of median stone size: $D_{50,\ initial}$.

These parameters are used as an input for Eq. (15). In Eq. (15), $\tau_{cr,pred}$ represents the required critical bed shear-stress of the stone size $D_{67.5}$ of the top layer; τ_c represents the current induced bed shear-stress and is calculated using Eqs. (A.1), (A.2) and (A.3); τ_w represents the wave induced bed shear-stress, calculated by using $H_{1/10}$ and T_p in Eqs. (A.6), (A.10) and (A.12). $H_{1/10}$ can be determined as $1.27H_s$. Both for the calculation of τ_c and τ_w, the bottom roughness $k_s = 2.5D_{50}$; s is the relative density of the stones (ρ_s/ρ_w) and g is the gravitational acceleration.

Eq. (14) can be used to calculate the critical bed shear stress $\tau_{cr,top\ \ layer}$ of the top layer, starting from the initial estimate of $D_{67.5}$. The initial estimate of the value of $D_{67.5}$ can be derived from the initial estimate for $D_{50,\ initial}$ and the knowledge of D_{85}/D_{15} (assuming a linear variation of the stone sizes in a semi-log diagram):

$$\log\left(\frac{D_{67.5}}{D_{50}}\right) = \frac{(67.5-50)}{(85-15)}\log\left(\frac{D_{85}}{D_{15}}\right) = 0.25\log\left(\frac{D_{85}}{D_{15}}\right). \tag{17}$$

Eq. (14) can then be used to calculate the critical bed shear stress $\tau_{cr,top\ \ layer}$ of the top layer by assuming $\theta_{cr} = 0.035$ and a value $D_{67.5}$ instead of D_{50}.

Another possibility is to calculate $\tau_{cr,pred}$ and $\tau_{cr,top\ layer}$ for different values of D_{50} (and $D_{67.5}$) as shown in Fig. 16 for an example

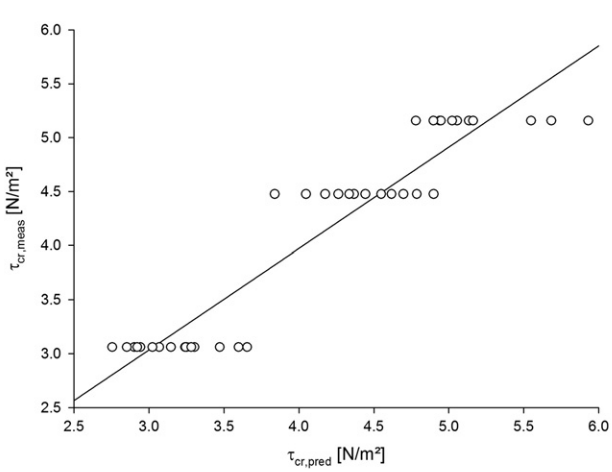

Fig. 12. Predicted value $\tau_{cr,pred}$ against measured value $\tau_{cr,meas}$, Eq. (13).

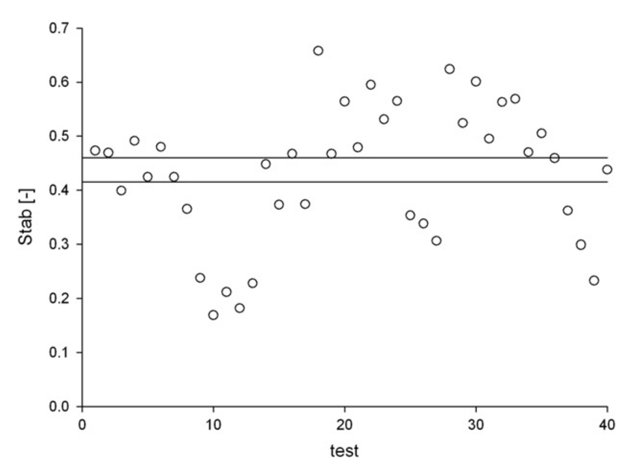

Fig. 13. OPTI-PILE parameter *Stab* (HR Wallingford Ltd for E-Connection Project BV) for the present data set.

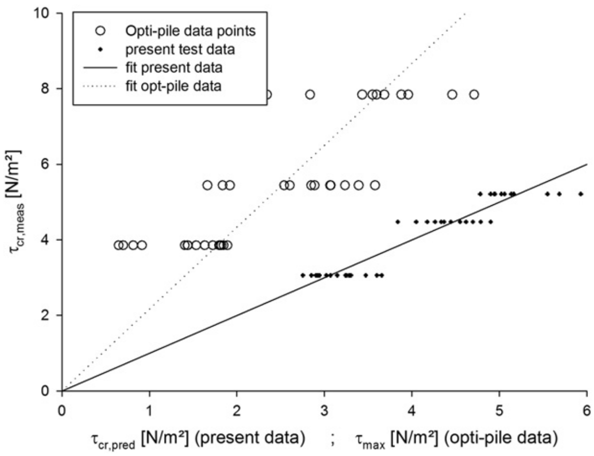

Fig. 14. Comparison of scatter for OPTI-PILE calculation (HR Wallingford Ltd for E-Connection Project BV) with present data set: measured value $\tau_{cr,meas}$ is plotted against $\tau_{cr,pred}$ (present data set) and τ_{max} (OPTI-PILE data).

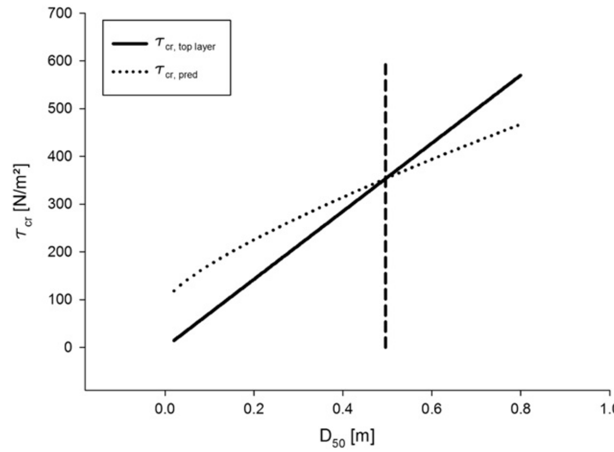

Fig. 16. Example: $d=20$ m, $U_c=1.5$ m/s, $D_{85}/D_{15}=2.5$, $H_s=6.5$ m and $T_p=11.2$ s. Comparison of $\tau_{cr,top\ layer}$ and $\tau_{cr,pred}$ as a function of D_{50}. $D_{50,stable}=0.496$ m.

case where $d=20$ m, $U_c=1.5$ m/s, $D_{85}/D_{15}=2.5$, $H_s=6.5$ m and $T_p=11.2$ s.

4.5. Comparison of the results with OPTI-PILE study

For the OPTI-PILE project (Section 2.2.2) a comparable approach was used as described in Section 4.2. The parameters which were used in the analysis presented in this paper, τ_w and τ_c, are comparable to the use of the OPTI-PILE parameter *Stab* (Eq. (9)). It was found that initiation of stone movement occurs when *Stab* exceeds the value 0.415. Although the results are based on irregular wave tests, the possibility exists to calculate the value of *Stab* for regular waves as well with the OPTI-PILE DESIGN TOOL V2.4 (HR Wallingford Ltd for E-Connection Project BV). The parameter *Stab* was calculated by HR Wallingford for the test series given in Table 2.

Fig. 13 plots this calculated values of Stab against the test no. The limits, which are defined in the OPTI-PILE projects as the transition between no movement and movement without failure (*Stab* = 0.415) and the transition between movement without failure and failure

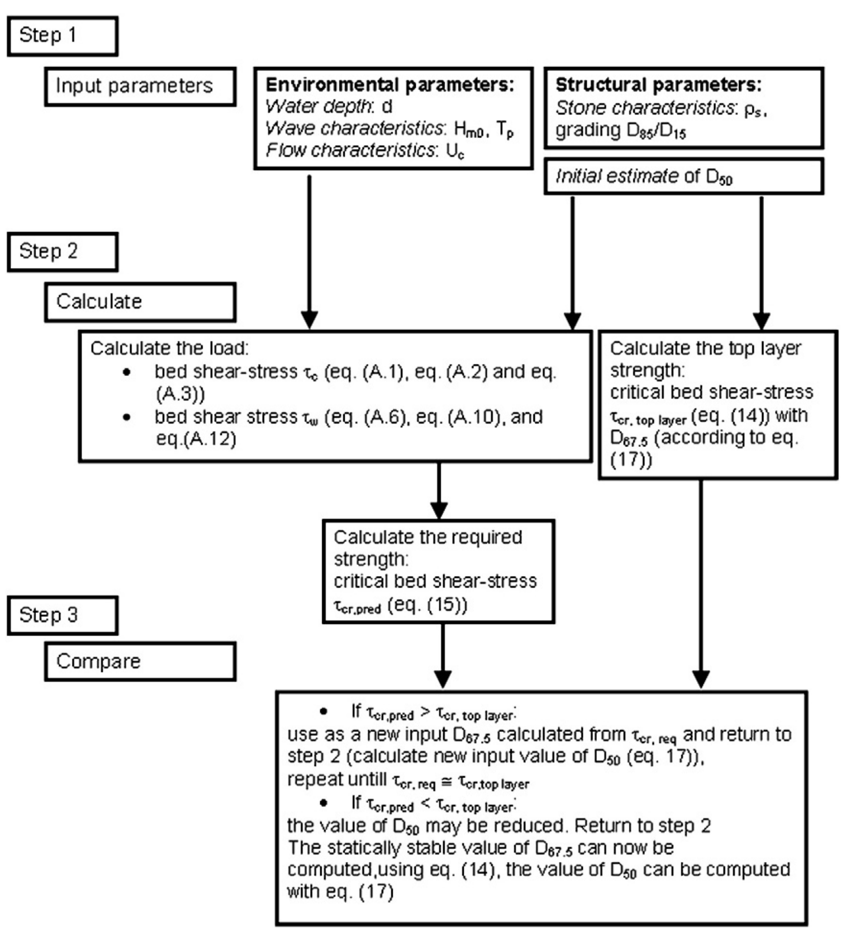

Fig. 15. Design tree for statically stable scour protection.

($Stab = 0.46$) are plotted as a full line in the figure. As all present tests represent initiation of movement, a value of $Stab \cong 0.415$ would be expected. From Fig. 13, it can be decided that the parameter *Stab* cannot be used to represent the initiation of movement for the present test series.

In Fig. 14 the required stone size using the OPTI-PILE parameter *Stab* is compared with the proposed design formula (Eq. (13)). For the OPTI-PILE data set, τ_{max} (Eq. (A.21)) is plotted against the value of $\tau_{cr,meas}$. The points from the present data set (Fig. 12) are added to Fig. 14 by plotting the values of $\tau_{cr,pred}$ against the values of $\tau_{cr,meas}$. The difference between the values of $\tau_{cr,meas}$ used for the OPTI-PILE points and the values of $\tau_{cr,meas}$, used for the present study results from a different assumption for the value θ_{cr}. A value of $\theta_{cr} = 0.056$ is used in OPTI-PILE, while a value of 0.035 is used in this paper. This however only results in a difference by a constant factor. Furthermore, the value of $D_{67.5}$ is used in this thesis to calculate $\tau_{cr,meas}$, while D_{50} is used for the OPTI-PILE parameter.

From Fig. 14, it can be seen that

- the spreading around the value of τ_{max}, used in the OPTI-PILE project is much higher than the spreading around the predicted value, obtained with Eq. (13) or (15).
- a serious deviation from the regression line is obtained, when a linear regression through the origin is used for the OPTI-PILE parameter. This is due to the fact that the value of D_{50} is used instead of $D_{67.5}$ to calculate τ_{max}.

5. Application of the new prediction formula

In this section, the required stone size for a scour protection around a monopile foundation and a typical situation in the North Sea is calculated with different methods. The methods which are used are:

- the traditional approach, in which the amplified combined current and wave bed shear-stress determine the critical bed shear-stress. The amplification factor α for the bed shear stress is varied between a value of 2, 3 and 4 to account for the influence of the pile. Typically a value of 4 is used for a steady current and a value of 2.2 to 2.5 is used for waves. A value of $\theta_{cr} = 0.056$ is used for the critical Shields parameter. Two approaches are used to calculate the bed shear stress. The first method is the method according to Fredsøe and Deigaard (1992), in this case the bed shear stress τ_m according to Eq. (A.16) is applied, with f_w according to Eq. (A.11). Secondly the method according to Soulsby (1997) is used, Eqs. (A.21) and (A.15). In this case, the value of τ_{max} is applied, according to the recommendations of Soulsby (1997).
- the new prediction formula which aims for a static design, derived in Section 4.1: Eq. (15).
- Eqs. (7) and (8) given by Soulsby (1997), which calculate a critical stone size for the two separate loading conditions: wave loading and steady flow. No interaction between waves and current is considered. The amplification factor α for the bed shear stress is varied between a value of 2, 3 and 4 to account for the influence of the pile, both for the steady flow as for the wave induced flow velocity.

The OPTI-PILE parameter's calculation is bound to confidentiality and can therefore not be included in this calculation.

A monopile foundation is to be installed in a water depth of 20 m. The pile diameter is 5 m. The design wave conditions have a significant wave height $H_{m0} = 6.5$ m. The corresponding peak wave period $T_p = 4.4\sqrt{H_{m0}} = 11.2$ s. The tidal velocity has an average value $U_c = 1.5$ m/s. To calculate Eq. (15), D_{85}/D_{15} is assumed to be equal to 2.5. In Table 4, the comparison is made between the required scour protection stone size for several calculation methods. It shows that a significantly smaller stone size can be obtained when using Eq. (15) instead of the traditional approach, when using typical values for α. As can be seen in Table 4, the result of the traditional methods is strongly depending on the choice of the amplification factor α.

Table 4
Comparison between required stone size (D_{50} [m]) according to different calculation methods: $d = 20$ m; $H_{m0} = 6.5$ m; $T_p = 11.2$ s; $U_c = 1.5$ m/s; $D_{85}/D_{15} = 2.5$.

Amplification α	Traditional approach according to Fredsoe and Deigaard, use of τ_m	Traditional approach according to Soulsby, use of τ_{max}	Soulsby (1997), waves	Soulsby (1997), current	De Vos, static approach
2	0.68	0.66	0.29	0.013	0.496
3	1.30	1.51	0.55	0.022	0.496
4	1.97	2.75	0.85	0.033	0.496

6. Conclusion

In this paper, the experimental research which was performed to determine the required stone size for the top layer of a scour protection around a monopile foundation is discussed. A static design approach is used, leading to a scour protection for which no stones of the top layer move during a design storm.

The experiments were performed with regular waves and a steady current. The required stone size was determined as the stone size which is on the threshold of motion under the design loading conditions. The experimental results lead to a proposed design formula (Eq. (15)), which relates the required critical bed shear-stress τ_{cr} – representing the resistance of the stones to movement – to the current and wave induced bed shear-stresses τ_c and τ_w, which represent the load which acts on the scour protection. By using an adjusted value for the wave-induced bed shear-stress, the proposed design formula is adjusted to be valid for irregular waves as well.

When comparing the proposed design formula to the existing design methods, a reduction in required stone size can be achieved when typical values of the amplification factor are used. It is advised to compare the results obtained with Eq. (15) with other data sets or field measurements when possible.

Acknowledgements

The author gratefully acknowledges the Research Foundation — Flanders for the grant which was provided for her research at Ghent University.

Appendix A. Computation of bed shear-stress

A.1. Steady uniform flow

For a steady, uniform flow, the bed shear-stress τ_c is defined as:

$$\tau_c = \frac{1}{2}\rho_w f_c U_c^2 \tag{A.1}$$

with f_c a dimensionless friction coefficient of the bed, determined as (Liu, 2001):

$$f_c = \frac{2g}{C^2} = \frac{2g}{\left(\frac{\sqrt{g}}{\kappa}\ln\left(\frac{d}{z_0 e}\right)\right)^2} \tag{A.2}$$

with C the Chézy coefficient [$\sqrt{m}/s$]; z_0 the roughness length, corresponding to the elevation above the bed with zero velocity (Eq. (A.3)); $\kappa = 0.4$, the Von Karman constant; ν the kinematic viscosity of water ($= 10^{-6}$ m^2/s) and $e = 2.718$.

Colebrook and White (1937) studied pipe flows and a comparison of their results with the results from Nikuradse led to:

$$z_0 = \frac{k_s}{30} + \frac{\nu}{9u_*}. \tag{A.3}$$

This equation simplifies to the well-known value for a hydraulically rough flow:

$$z_0 = \frac{k_s}{30}, \quad \frac{u_* k_s}{\nu} \geq 70 \tag{A.4}$$

and in case of a hydraulically smooth flow:

$$z_0 = \frac{\nu}{9u_*}, \quad \frac{u_* k_s}{\nu} \leq 5. \tag{A.5}$$

The value of the bottom roughness k_s depends on the presence of ripples: a widely used value when no ripples are present is $k_s = 2.5d_{50}$, with d_{50} the median sediment grain diameter. When ripples are present, $k_s = (0.5–1)H_r$, with H_r the ripple height (Liu, 2001).

A.2. Wave induced bed shear-stress

In the case of waves, the bed shear-stress is oscillatory and has an amplitude τ_w which is obtained through the use of a wave friction factor f_w:

$$\tau_w = \frac{1}{2}\rho_w f_w U_m^2 \tag{A.6}$$

with U_m the amplitude of this horizontal velocity just above the bed, which can, for monochromatic waves, be derived with linear wave theory as:

$$U_m = \frac{\pi H}{T_w} \cdot \frac{1}{\sinh\left(\frac{2\pi d}{L}\right)} \tag{A.7}$$

in which H represents the wave height, T_w is the wave period, d is the water depth and L is the wave length.

Several expressions for the wave friction factor f_w exist. Nielsen (1992), Fredsøe and Deigaard (1992), Soulsby (1997) and Dixen et al. (2008) are cited here. The wave friction factor has a dominant role in the combined wave and current climate and a correct estimate of its value is important.

Fredsøe and Deigaard (1992) calculate a theoretical solution for the wave friction factor over a rough bed with a momentum method, obtaining a theoretical expression for the wave friction factor f_w and the wave boundary layer thickness δ:

$$f_w = 0.04\left(\frac{A}{k_s}\right)^{-1/4}, \quad \frac{A}{k_s} > 50 \tag{A.8}$$

$$\frac{\delta}{k_s} = 0.09\left(\frac{A}{k_s}\right)^{0.82} \tag{A.9}$$

with k_s the sediment roughness and A the amplitude of the wave orbital motion at the bed:

$$A = \frac{U_m T_w}{2\pi}. \tag{A.10}$$

In case of small values of the ratio of the orbital amplitude to the bottom roughness A/k_s, the approximation suggested by Kamphuis is withheld for the wave friction factor:

$$f_w = 0.4\left(\frac{A}{k_s}\right)^{-0.75}, \quad \frac{A}{k_s} < 50. \tag{A.11}$$

A recent study of Dixen et al. (2008) suggests an adjustment to f_w and δ for small values of A/k_s, based on new experimental results:

$$f_w = 0.32\left(\frac{A}{k_s}\right)^{-0.8}, \quad 0.2 < \frac{A}{k_s} < 10 \tag{A.12}$$

$$\frac{\delta}{k_s} = 0.08\left(\left(\frac{A}{k_s}\right)^{0.82} + 1\right), \quad 0.5 < \frac{A}{k_s} < 5000. \tag{A.13}$$

Nielsen (1992) suggests Eq. (A.14) for the wave friction factor in case of a rough turbulent flow:

$$f_w = \exp\left[5.5\left(\frac{k_s}{A}\right)^{0.2} - 6.3\right]. \tag{A.14}$$

Soulsby (1997) gives expression (A.15) for the wave friction factor in the case of a rough bed:

$$f_w = 1.39\left(\frac{A}{z_0}\right)^{-0.52} \tag{A.15}$$

for all values of A/k_s, with z_0 the bed roughness length $= d_{50}/12$ for hydrodynamical rough flows.

In general, a sand bed exposed to waves will be hydraulically rough, when the waves are sufficiently large for the sediment to move. Moreover, a scour protection is also hydraulically rough. For this reason, only the equations for a rough bed are mentioned here.

A.3. Bed shear-stress in combined wave and current climate

In most marine environments, both currents and waves occur simultaneously. Difficulties arise because they interact, so that their combined influence is not the same as a linear sum of their separate influences. Several different theories and models have been proposed to calculate the bed shear-stress τ_{wc} in combined waves and current, leading to considerable differences in the predicted bed shear-stress. Some of these are summarized below.

Fredsøe and Deigaard (1992) suggest for the case where waves coexist with a weak, parallel current that the boundary layer thickness is determined by the wave motion only (Eq. (A.9) or (A.13)). This results in a mean bed shear-stress τ_m:

$$\tau_m = \frac{2}{\pi}\rho_w f_w U_m U_\delta \tag{A.16}$$

with

$$U_\delta = C - \sqrt{C^2 - U_c^2} \tag{A.17}$$

and

$$C = U_c + \frac{1}{\pi} f_w U_m \left(6.2 + \frac{1}{\kappa}\ln\left(\frac{d}{30\delta}\right)\right)^2 \tag{A.18}$$

in which U_c represents the average current velocity; f_w is the wave friction factor according to Eq. (A.8), (A.11) or (A.14); U_m according to Eq. (A.7); δ according to Eq. (A.9) or (A.13), d the water depth and $\kappa = 0.4$, the Von Karman constant.

The resulting maximum bed shear-stress according to Fredsøe and Deigaard (1992) is:

$$\tau_{max} = \frac{1}{2}\rho_w f_w (U_m + U_\delta)\cdot|U_m + U_\delta| \tag{A.19}$$

with U_m according to Eq. (A.7) and U_δ according to Eq. (A.17).

Soulsby (1997) compared the mean (τ_m) and maximum (τ_{max}) bed shear-stresses during a wave cycle. Based on a data set of 131 points two simple equations are derived, which according to Soulsby (1997) give an almost as good fit as the best theoretical models:

$$\tau_m = \tau_c\left[1 + 1.2\left(\frac{\tau_w}{\tau_c + \tau_w}\right)^{3.2}\right] \quad (A.20)$$

$$\tau_{max} = \left[(\tau_m + \tau_w \cos\phi)^2 + (\tau_w \sin\phi)^2\right]^{1/2} \quad (A.21)$$

with ϕ the angle between the wave and current direction, τ_c determined according to Eq. (A.1) and τ_w determine according to Eq. (A.6).

According to Soulsby (1997), the calculation of τ_m is necessary to determine sediment diffusion, whereas the calculation of τ_{max} is necessary to determine the threshold of motion.

References

Baker, C.J., 1979. The laminar horseshoe vortex. Journal of Fluid Mechanics 95, 347–367.
Ballast Nedam, Oud, J.C., 2002. Foundation Design Monopile — Comparison Extra Steel Consumption Versus Scour Protection — 3.6 & 6.0 MW Wind Turbines, DOWEC, Amstelveen.
Breusers, H.N.C., Raudkivi, A.J., 1991. Scouring. Balkema.
Cefas, 2006. Scroby sands offshore wind farm — coastal processes monitoring. Final Report for the Department of Trade and Industry. Contract AE0262, Cefas Lowestoft Laboratory, Suffolk.
CEM, US Army Corps of Engineers, 2002. Coastal Engineering Manual 1110-2-1100, Washington, D.C.
Chiew, Y.M., 1995. Mechanics of riprap failure at bridge piers. Journal of Hydraulic Engineering 121 (9), 635–643.
CIRIA/CUR, 1991. Manual on the Use of Rock in Coastal and Shoreline Engineering. CUR 154.
Colebrook, C.F., White, C.M., 1937. Experiments with Fluid Friction in Roughened Pipes. Proceedings of the Royal Society of London. Series A, Mathematical and Physical Sciences 161 (906), 367–381.
Dargahi, B., 1989. The turbulent flow field around a circular cylinder. Experiments in Fluids 8 (1), 1–12.
den Boon, J.H., Sutherland, J., Whitehouse, R., Soulsby, R., Stam, C.J.M., Verhoeven, K., Høgedal, M., Hald, T., 2004. Scour Behaviour and Scour Protection for Monopile Foundations of Offshore Wind Turbines, European Wind Energy Conference & Exhibition (EWEC), London, UK.
De Vos, L., 2008. Optimisation of Scour Protection Design for Monopiles and Quantification of Wave Run-up. Engineering the Influence of an Offshore Wind Turbine on Local Flow Conditions. PhD Thesis, Ghent University, Ghent, pp 319.
De Vos, L., De Rouck, J., Troch, P., Frigaard, P., in preparation. Empirical design of scour protections around monopile foundations. Part 2: Dynamic approach.
Dixen, M., Hatipoglu, F., Sumer, B.M., Fredsøe, J., 2008. Wave boundary layer over a stone-covered bed. Coastal Engineering 55 (1), 1–20.
E-Connection, Vestas Wind Systems, D.K., Germanischer, Lloyd, Windenergie, D., 2002–2004. OPTI-PILE, Fifth Research and Technological Development Framework Programme.
Fredsøe, J., Deigaard, R., 1992. Mechanics of Coastal Sediment Transport. Advanced Series on Ocean Engineering, Vol. 3. World Scientific.
Grune, J., Sparboom, U., Schmidt-Koppenhagen, R., Wang, Z., Oumeraci, H., 2006. Stability Tests of Geotextile Sand Containers for Monopile Scour.
Hansen, N.-E.O., Gislason, K., 2005. Movable Scour Protection on Highly Erodible Sea Bottom, International Coastal Symposium.
Herman, S.A., Kooijman, H.J.T., Hendriks, H.B., van de Brug, E., Nedam, B., op den Velde, W., Van Oord, A.C.Z., van den Berg, R., Holland, L.M.G., 2003. Variations on a 500 MW Offshore Wind Farm Design, Offshore Wind Energy in the Mediterranean and Other European Seas Naples, Italy.
Hjorth, P., 1975. Studies on the Nature of Local Scour. Institute of Technology, Dept. of Water Resources Engineering.
Hoffmans, G.J.C.M., Verheij, H.J., 1997. Scour Manual. A.A. Balkema, Rotterdam, Netherlands; Brookfield, VT, xv. 205 pp.
Hofland, B., 2005. Rock & Roll: Turbulence-induced Damage to Granular Bed Protections. Department of Civil Engineering and Geosciences, Delft University of Technology.
Kirkegaard, L., Hebsgaard, M., Jensen, O.J., 1998. Design of scour protection for the bridge piers of the Øresund link. International Conference on Coastal Engineering, Copenhagen, Denmark, pp. 3634–3642.
Liu, Z., 2001. Sediment Transport, Aalborg.
Malarkey, Davis, 1998. Modelling wave-current interactions in rough turbulent bottom boundary layers. Ocean Engineering 25 (Nos. 2–3), 119–141.
May, R.W.P., Ackers, J.C., Kirby, A.M., 2002. Manual on Scour at Bridges and Other Hydraulic Structures. CIRIA.
Melville, B.W., Coleman, S.E., 2000. Bridge Scour. Water Resources Publications Highlands USA. 550 pp.
Melville, B.W., Raudkivi, A.J., 1977. Flow characteristics in local scour at bridge piers. Journal of Hydraulic Research 15 (4), 373–380.
Nielsen, P., 1992. Coastal Bottom Boundary Layers and Sediment Transport. : Advanced Series on Ocean Engineering, Vol. 4. World Scientific.
Shields, A., 1936. Anwendung der Aehnlichkeitsmechanik und der Turbulenzforschung auf die Geschiebebewegung. Preussische Versuchsanstalt für Wasserbau und Schiffbau.
Soulsby, R., 1997. Dynamics of Marine Sands: A Manual for Practical Applications. Thomas Telford.
Sumer, B.M., Christiansen, N., Fredsøe, J., 1997. The horseshoe vortex and vortex shedding around a vertical wall-mounted cylinder exposed to waves. Journal of Fluid Mechanics 332, 41–70.
Sumer, B.M., Fredsøe, J., 1997. Hydrodynamics Around Cylindrical Structures. Advanced Series on Ocean Engineering. World Scientific, Singapore; River Edge, NJ. xviii, 530 pp.
Sumer, B.M., Fredsøe, J., 2002. The Mechanics of Scour in the Marine Environment. Advanced Series on Ocean Engineering. River Edge, N.J., World Scientific. 536 pp.
Umeda, S., Yuhi, M., Ishida, H., 2003. Numerical study of three-dimensional flow fields around the base of a vertical cylinder in oscillatory plus mean flow. Coastal Structures 2003 — Proceedings of the Conference. American Society of Civil Engineers, Reston, VA 20191-4400, United States, Portland, OR, United States, pp. 751–763.
Van Oord, A.C.Z., 2003. Scour Protection for 6 MW OWEC with Monopile Foundation in North Sea. Gorinchem.
Whitehouse, R., 1998. Scour at Marine Structures: A Manual for Practical Applications. Thomas Telford, London. xix, 198 pp.
Whitehouse, R.J.S., Sutherland, J., O'Brien, D., 2006. Seabed scour assessment for offshore windfarm. International Conference on Scour and Erosion. Nanyang University, Nanyang, Singapore.